

# Preparation and characterization of silica sol/fluoroacrylate core–shell nanocomposite emulsion

Li Wang · Xiaolong Li · Mingfu Huang ·  
Zushun Xu · Changfeng Yi

Received: 15 November 2011 / Accepted: 14 March 2012 / Published online: 27 March 2012  
© Iran Polymer and Petrochemical Institute 2012

**Abstract** The silica sol/fluoroacrylate core–shell nanocomposite emulsion was successfully synthesized via traditional emulsion polymerization through grafting of KH-570 onto silica particles. Comparing the performance of the polyacrylate copolymer, the fluorinated polyacrylate copolymer and the silica sol/fluoroacrylate core–shell nanocomposite emulsion, we can come to a conclusion that the silica sol/fluoroacrylate core–shell nanocomposite emulsion presents significantly excellent performance in all aspects. The products were characterized by Fourier transform infrared (FTIR), photon correlation spectroscopy (PCS), transmission electron microscopy (TEM), thermogravimetry (TGA), Contact angle and UV–vis analyses techniques. The chemical structure of polyacrylate copolymer, fluorinated polyacrylate copolymer and silica sol/fluoroacrylate nanocomposite were detected by FTIR. The size and stability of emulsion latex particles were determined by PCS technique. TEM analysis confirmed that the resultant latex particle has the core–shell structure, obviously. The water absorption and contact angle data also showed that the silica sol/fluoroacrylate nanocomposite film has good hydrophobic performance. TGA analysis indicated the weight loss of the silica sol/fluoroacrylate nanocomposite film begins at around 350 °C which testifies its good thermal stability. The UV–vis spectroscopy analysis showed that the silica sol/fluoroacrylate nanocomposite film possess UV–vis shielding effect

when the added volume amount of KH570 modified silica sol is up to 5 mL. Therefore, the excellent properties of hydrophobicity, thermodynamics and resistance to ultra-violet provide the silica sol/fluoroacrylate nanocomposite film with potential applications in variety fields. In addition, the formation mechanism of core–shell structure silica sol/fluoroacrylate nanocomposite latex particles was speculated.

**Keywords** Silica sol/fluoroacrylate nanocomposite emulsion · Core–shell structure · Stability · Hydrophobic performance · UV–vis shielding effect

## Symbols and abbreviations

KH-570	3-(Trimethoxysilyl) propyl methacrylate
FTIR	Fourier transform infrared spectrometer
PCS	Photon correlation spectroscopy
TEM	Transmission electron microscopy
TGA	Thermogravimetric analysis
UV–vis analysis	UV–visible analysis
St	Styrene
<i>n</i> -BA	<i>n</i> -Butyl acrylate
DFHMA	Dodecafluoroheptyl methacrylate
HEMA	2-Hydroxyethyl methacrylate
TEOS (Si(OC <sub>2</sub> H <sub>5</sub> ) <sub>4</sub> )	Tetraethoxysilane
SDS	Dodecyl sodium sulfate
OP-10	Polyoxyethylene alkylphenol ether
NaHCO <sub>3</sub>	Sodium hydrogen carbonate
NH <sub>3</sub> ·H <sub>2</sub> O	Ammonium hydroxide
KPS (K <sub>2</sub> S <sub>2</sub> O <sub>8</sub> )	Potassium peroxydisulfate
CaCl <sub>2</sub>	Calcium chloride
<i>D<sub>w</sub></i>	Weight-average diameter
PDI	Polydispersity index

L. Wang · X. Li · M. Huang · Z. Xu · C. Yi (✉)  
Ministry-of-Education Key Laboratory for the Green Preparation and Application of Functional Materials, Hubei University, Youyi Road 368#, Wuchang District, Wuhan 430062, Hubei, People's Republic of China  
e-mail: ChangfengYi63@yahoo.com.cn



## Introduction

In recent years, organic–inorganic nanocomposite systems have attracted great attention due to their unique properties to combine the remarkable advantages of inorganic materials with those of organic materials [1–4], making them to possess superior properties such as mechanical [5, 6], thermal [7], optical [8, 9], electrical, and magnetic [10] properties with extensive potential applications in various fields, ranging from paints, magnetic fluids, electronics, and high-quality paper coating to catalysis, microelectronics, diagnostics and biotechnology [11]. Inorganic particles which have strong adhesion with polymer matrix in terms of small particle size, high specific surface and thermal stability can improve the rigidity, hardness and abrasion resistance of polymers.

On the other hand, organic polymer materials with excellent optical properties, good flexibility and toughness can improve the brittleness, dispersibility and stability of inorganic materials. In addition, the interfacial adhesion between the inorganic compound and the polymer can be improved by introducing chemical bonds between the organic and inorganic phases. One route for forming such chemically bonded organic–inorganic composite materials is to utilize the organic polymers functionalized with trialkoxysilane groups as the sol–gel precursors [12–14].

Fluoropolymers exhibit extraordinary properties such as good anti-chemical and thermostability, low friction coefficient, low flammability, excellent weatherability coupled with good resistance to oxidation, extremely low surface energy and related unwettability, and relatively low permeability for most gases [15–17], as well as excellent mechanical behavior [18–20]. It is due to the low polarizability and strong electronegativity of fluorine atoms [21–23] which were closely arranged outside of the backbone, providing shielding effect to ensure the stability of the copolymer.

Moreover, the outstanding properties of fluoropolymers, especially the low surface energy, have enhanced their application in many high-technology applications such as aerospace, microelectronics, paints, coatings, etc. The popular fluorinated acrylic polymers because of their unique properties, especially the acrylic main-chains, ensure that the polymers can adhere well to various matrices [23, 24] to improve wide applications [25–29] such as high-performance paints and varnishes in textile, paper, leather, construction, automotive and aerospace industries, as well as, optics and microelectronics.

But the fluoropolymers also have shortcomings, such as poor substrate-adhesion and intolerance to low temperature. However, it could be solved by introducing silicon-containing functional groups. Silicon-containing polymers represent attractive surface properties [30], low elastic-modulus, exceptionally low glass-transition temperature, as

well as, high thermal and chemical stability. Constructing a new polymer combining the unique properties of both fluorinated and silicated polymers can provide interesting new materials, particularly with regard to the potential for nonwetting surfaces with low surface energy [31]. For example, Xiong et al. [15] prepared the core–shell latexes with fluorine enriched in the shell by emulsion polymerization of a variety of hydrocarbon monomers with (perfluoroalkyl)methyl methacrylate and vinyltriethoxysilicone in the presence of a reactive anionic and a long-chain anionic-nonionic emulsifiers. He et al. [18] succeeded in synthesizing a novel fluorinated acrylic polymer with core–shell structure, obtained by semi-continuous seed emulsion polymerization and modified by hydrolysis of tetraethyloxysilane [TEOS,  $\text{Si}(\text{OC}_2\text{H}_5)_4$ ] in the presence of silane coupling agent dodecyltrimethoxysilane [DTMS,  $\text{C}_{12}\text{H}_{25}\text{Si}(\text{OCH}_3)_3$ ].

In this study, nanoscale silica sol was synthesized by Stöber method [32] and was modified with 3-(trimethoxysilyl)propyl methacrylate (KH-570) [33]. In the presence of a complex system of an anionic and a nonionic emulsifiers, the core–shell structure silica sol/fluoroacrylate nanocomposite emulsion was prepared by emulsion polymerization in water as the medium. This method avoids the cumbersome steps of synthesizing the fluorosilicone monomer and introduces chemical bond between organic and inorganic phase to improve their compatibility. In addition, compared with the work of Cui et al. [34] we discussed more application fields for the obtained material. Thus, the obtained product which combines the characteristics of fluorinated organic polymers and silica inorganic materials is supposed to have great potential in a more extensive application scope.

## Experimental

### Materials

Styrene (St) and *n*-butyl acrylate (*n*-BA) (Shanghai Chemical Reagents Co., China, chemical pure) were purified by distilled under vacuum, and then stored at  $-5\text{ }^\circ\text{C}$ . Dodecafluoroheptyl methacrylate  $\text{CH}_2 = \text{CHCOOCH}_2\text{CF}(\text{CF}_3)\text{CFHCF}(\text{CF}_3)_2$  (Actyflon-G04 or DFHMA) (XEOGIA Fluorine–Silicon Chemical Co., China, chemical pure) was distilled under reduced pressure before use. 2-Hydroxyethyl methacrylate (HEMA, analytical pure) was obtained from Fluka, Germany. Tetraethoxysilane [TEOS,  $\text{Si}(\text{OC}_2\text{H}_5)_4$ ] obtained from Aladdin Reagent (Shanghai, China). 3-(Trimethoxysilyl) propyl methacrylate (KH-570) supplied by Wuhan University Chemical (Wuhan, China). Dodecyl sodium sulfate (SDS), polyoxyethylene alkylphenol ether (OP-10), sodium hydrogen carbonate ( $\text{NaHCO}_3$ ), ammonium hydroxide ( $\text{NH}_3\cdot\text{H}_2\text{O}$ ,

25 wt %), potassium peroxodisulfate ( $K_2S_2O_8$ , KPS) and ethanol were all purchased in reagent-grade purity from Shanghai Chemical Reagent Co. (Shanghai, China). Potassium peroxodisulfate was purified by recrystallization in deionized water. In all polymerization and treatment processes, deionized water was used.

#### Preparation of the KH570-modified silica particles

Highly monodisperse  $SiO_2$  colloid particles were prepared through the well-known Stöber procedure [32]. 15 mL TEOS was slowly added into the mixture of 150 mL absolute alcohol, 15 mL deionized water and 1.5 mL ammonia under magnetic stirring at a speed of 200 rpm at room temperature for 24 h to obtain a clear light blue solution. The modification of the obtained colloidal silica with KH-570 was performed according to the Philipse and Vrij method [33]. At ambient temperature, 4.5 mL KH-570 was directly fed into the above obtained silica sol followed by strong magnetic stirring for 8 h. Then, the reaction solution was heated to 80 °C for 2 h to promote covalent bonding of the organosilane to the surface of the silica nanoparticles. Afterward, the mixture was cooled to room temperature and centrifuged at 8,000 rpm for 10 min to purify the KH570-modified  $SiO_2$ . After recentrifugation and redispersion as stated above for five times, the pure KH570-modified  $SiO_2$  was obtained.

#### Preparation of the silica sol/fluoroacrylate nanocomposite emulsion

The silica sol/fluoroacrylate nanocomposite emulsion was prepared by traditional emulsion polymerization. A certain amount of emulsifiers, polyoxyethylene alkylphenol ether (OP-10) and dodecyl sodium sulfate (SDS) (OP-10 Wt: SDS Wt = 1:1) were dissolved in deionized water, then the resultant mixture was homogenized by ultrasonic for

several times to obtain clarified solution. Then the clarified solution was transferred into a 100 mL four-neck glass flask equipped with reflux condenser, mechanical stirrer, separating funnel and inlet for nitrogen gas. At the same time, the monomers mixture of St, BA, HEMA, DFHMA and KH570-silica sol was fed into the flask. After continuous high-speed stirring for 1 h to obtain the pre-emulsion, the system was then heated and when the temperature of the system reached 70 °C, the KPS aqueous solution was dropwised into the flask at a rate of 12 droplet/min to initiate the polymerization. Finally, the temperature was maintained at 70 °C for another 8 h to obtain stable latex. The recipes for the preparation of silica sol/fluoroacrylate nanocomposite emulsion are shown in Table 1.

#### Preparation of the polyacrylate copolymer emulsion and the fluorinated polyacrylate copolymer emulsion

The general procedure was the same as describe above. The recipes for the preparation of polyacrylate copolymer emulsion and fluorinated polyacrylate copolymer emulsion are shown in Table 1.

#### Characterization of copolymer

##### Structural characterization

The emulsion was precipitated in the mixture of  $CaCl_2$  aqueous solution and methanol and the obtained precipitate was washed three times with ethanol and deionized water to remove surfactant. Finally, the precipitate was dried under vacuum at 60 °C for 24 h.

The chemical structure of the samples was identified by FTIR recorded on a Perkin-Elmer Spectrum One FTIR Spectrometer, USA. The samples for FTIR analysis were mixed with KBr powder and pressed into pellets.

**Table 1** Recipes of emulsion polymerization process

Components (g)	1	2	3	4	5	6	7
HEMA	0.625	0.3125	0.3125	0.3125	0.3125	0.3125	0.3125
DFHMA	0	0.3125	0.3125	0.3125	0.3125	0.3125	0.3125
KH570-silica	0	0	1	3	5	7	9
St	1.875	1.875	1.875	1.875	1.875	1.875	1.875
BA	3.75	3.75	3.75	3.75	3.75	3.75	3.75
OP-10	0.125	0.125	0.125	0.125	0.125	0.125	0.125
SDS	0.125	0.125	0.125	0.125	0.125	0.125	0.125
KPS	0.0625	0.0625	0.0625	0.0625	0.0625	0.0625	0.0625
$NaHCO_3$	0.08	0.08	0.08	0.08	0.08	0.08	0.08
Deionized water	25	25	25	25	25	25	25

Sample No. 1 is sample a; Sample No. 2 is sample b; Sample No. 3 is sample c



### Particle size characterization

The size and distribution of emulsion latex particles were determined by photon correlation spectroscopy (PCS) detector from Malvern, UK. The measure temperature was fixed at 25 °C and the scattering angle was fixed at 90°. Before the test, the samples were diluted at a ratio of 1:200 to prevent multiple scattering.

### Transmission electron microscopy (TEM)

The morphology of silica sol and silica sol/fluoroacrylate nanocomposite emulsion latex particle was characterized by transmission electron microscopy (TEM) on a Tecnai G20 transmission electron microscope FEI, USA. Before observation, one drop of the emulsion was diluted into water and placed on a carbon-coated copper grid dried in air.

### Stability of the emulsion

The storage stability of emulsion was symbolized by storing the emulsion at room temperature. With the lapse of time, the fewer the precipitation, the better was the storage stability of the emulsion. To test the dilution stability of the emulsion, 1 mL of polymer emulsion was poured into 9 mL of deionized water to dilute ten times and sealed in a tube for 72 h, to observe whether the dilution emulsion shows the stratification phenomenon or not. Heat-resistance and cold-resistance of the emulsion were tested by keeping the emulsion samples at 60 and −5 °C for 48 h, respectively. Then, the samples were observed whether the stratification occurred or not.

### Thermal stability

A Perkin-Elmer TGA-7 (USA) was used to detect the thermal stability of the emulsion films under nitrogen atmosphere from room temperature to 800 °C at a heating rate of 10 °C/min.

### Film formation and characterization

The tested films were prepared by putting a certain amount of the emulsion into dry clean petri dishes and drying for several days at room temperature or drying at 50–60 °C for several hours.

### Water resistance of emulsion films

Water resistance of emulsion films was symbolized by water absorption of films which measured by gravimetric variation before and after immersing the films into

deionized water for 72 h. Certain amount of emulsion membrane (written as  $W_0$ ) was put it into deionized water for 72 h at room temperature, and was taken out and filtered rapidly, then dried and weighed, the final quantity was written as  $W_1$ . Water absorption of the emulsion membrane was calculated according to the following formula:

$$\text{Water absorption (\%)} = [(W_1 - W_0)/W_0] \times 100 \quad (1)$$

### Contact angle

Dynamic contact angle of water on the emulsion films was determined by a Krüss K-12 contact-angle analysis instrument (Krüss Co., Germany) at 25 °C. Cut emulsion membrane into rectangle spline samples (2 × 1 cm) and placed them into the clip set of the instrument. The wetting circumference was first measured in *n*-hexane and the contact angle was then measured with water as the test liquid.

### UV-vis spectroscopies

The UV-vis optical transmission spectra were recorded by a  $\lambda$ -17 UV-vis recording spectrophotometer (Perkin Elmer, USA) and the range of the scanning was from 200 to 800 nm.

## Results and discussion

### FTIR spectra

The chemical structure of polyacrylate copolymer, fluorinated polyacrylate copolymer and silica sol/fluoroacrylate nanocomposites are detected by FTIR and the results are presented in Fig. 1. In all of the three spectra, the characteristic absorption peak of the C=C bond at 1,620–1,680  $\text{cm}^{-1}$  disappears, indicating that the monomers were polymerized. All the spectra exhibit the characteristic stretching vibration band of O–H at 3,442  $\text{cm}^{-1}$ , stretching bands of C–H ( $\text{CH}_2$ ) at 2,959 and 2,873  $\text{cm}^{-1}$ , stretching vibration band of C=O at 1,725  $\text{cm}^{-1}$ , and symmetric stretching vibration peak of C–O at 1,163  $\text{cm}^{-1}$ . The typical stretching vibration bands of the C=C bonds in the benzene rings are at 1,454, 1,494 and 1,602  $\text{cm}^{-1}$ . The characteristic stretching bands of mono-substituted benzene ring are obviously shown at 698 and 760  $\text{cm}^{-1}$ . Compared with the FTIR spectrum a in Fig. 1, when the fluorinated acrylate is introduced into the system, the FTIR absorption peaks at 1,000–1,200  $\text{cm}^{-1}$  in the spectrum b in Fig. 1 are wider and blunter. It can be attributed to the overlap of the stretching vibration bands of C–F bond and the stretching vibration absorption bands of the C–O–C



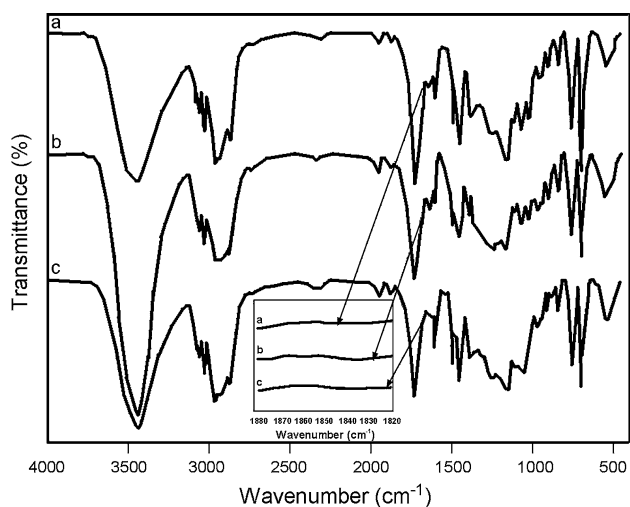


**Fig. 1** FTIR spectra of polyacrylate copolymer (a), fluorinated polyacrylate copolymer (b) and silica sol/fluoroacrylate nanocomposite (c): the inset figure is the enlargement of the characteristic absorption peak of the C=C bond

bond. Furthermore, the introduction of the modified silica sol makes the absorption peak at  $1,000\text{--}1,100\text{ cm}^{-1}$  to be wider due to the characteristic stretching band of Si–O. Accordingly, FTIR spectrum c in Fig. 1 confirms the formation of silica sol/fluoroacrylate nanocomposite. Figure 1 reveals that all the monomers have taken part in the polymerization process.

#### Size and morphology of the latex particles

##### Particle size of the latex particles

According to the Fig. 2, PCS analysis indicates that the obtained latex particles prepared by the conventional emulsion polymerization are uniform with  $100\text{--}200\text{ nm}$  in diameter and possess narrow size distributions. In addition, we can conclude that the size of silica sol/fluorinated-containing latex particles is larger than the other systems. Under the same recipe conditions, KH570-silica sol as monomer is added to the system and the micelles forms are larger than the other systems. And more importantly, the cross-link effect of the KH570-silica sol also makes the size of the silica sol/fluorinated-containing latex particles is larger than the other systems.

Figure 3 illustrates the effects of the volume amount of KH570-silica sol (concentration of KH570-silica sol is  $0.4\text{ mol/L}$ ) on  $D_w$  (weight-average diameter) and PDI (the polydispersity index) of the latexes prepared by traditional emulsion polymerization. As shown in Fig. 3, silica sol/fluoroacrylate nanocomposite emulsion latex particle size increases gradually with the increase in the content of KH570-silica sol. When the volume amount of KH570-silica sol was up to  $9\text{ mL}$ , the size of the latex increased to  $300\text{--}400\text{ nm}$ ,

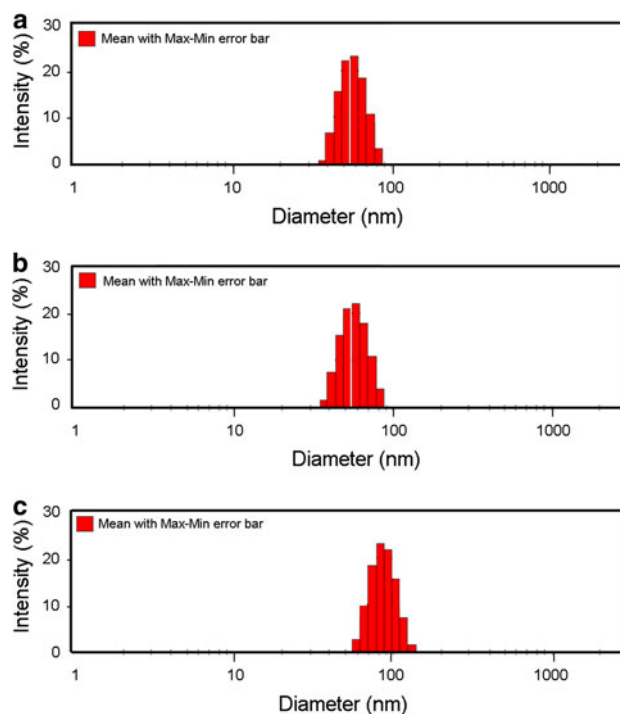


**Fig. 2** Particle size intensity statistics of the polyacrylate copolymer latex (a), fluorinated polyacrylate copolymer latex (b), and silica sol/fluoroacrylate nanocomposite latex (c)

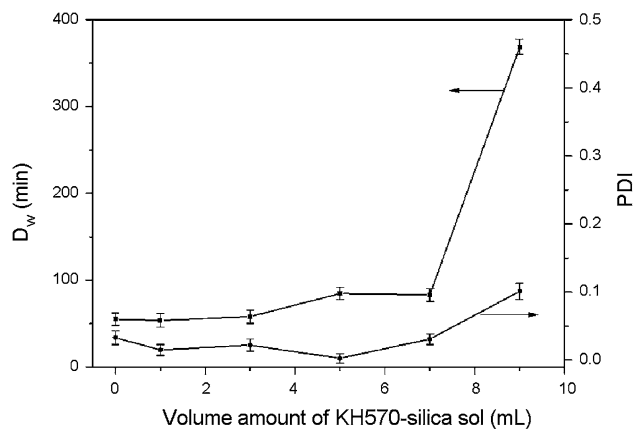


**Fig. 3** Effects of the amount of KH570-silica sol on  $D_w$  and PDI of latexes

suddenly. It may contribute to that when the content of the KH570-silica sol is high, it tends to form chemically cross-linked polymer on the particles. Therefore, the latex particle size increases gradually with the increase in the content of KH570-silica sol. Furthermore, all the latex particles possess narrow size-distribution with PDI lower than  $0.1$ .

##### Morphology of the latex particles

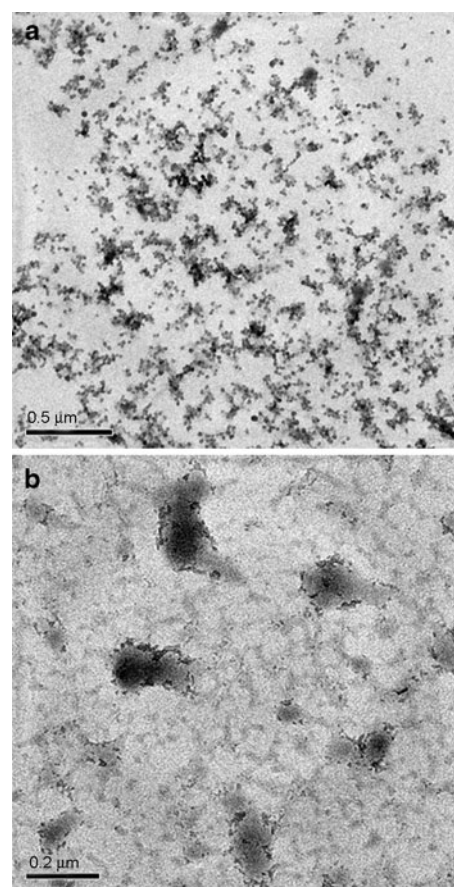
The formation mechanism of the silica sol/fluoroacrylate core-shell latex particle is speculated. As shown in

Scheme 1, SiO<sub>2</sub> colloid particles which contain the reactive hydroxyl on the surface are prepared by the hydrolysis and condensation of TEOS in the medium of ammonia and absolute ethanol with a sol–gel method at room temperature. The modification of the obtained colloidal silica with KH-570 begins with the hydrolysis of KH-570 to form hydroxyl on the surface similar to the hydrolysis of TEOS at ambient temperature. Then, the system is heated to 80 °C to promote covalent bonding of the organosilane to the surface of the silica colloid particles by the condensation of hydroxyl.

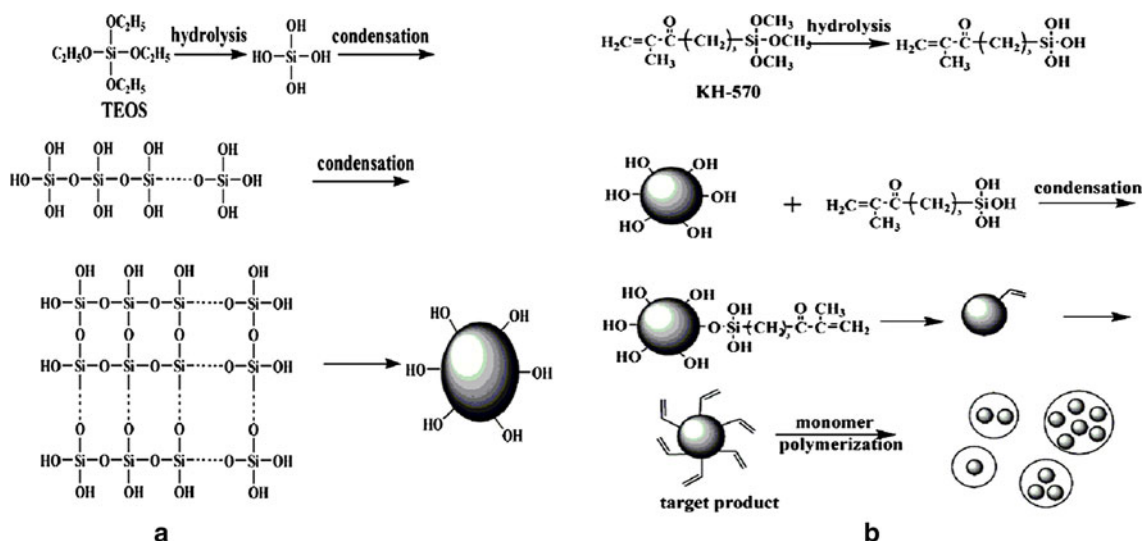
Finally, the target product which has many reactive double bonds on the surface was prepared as showed in Scheme 1b. Thus, when the target product joins in the system as monomer, one or more of the target product is emulsificated in the latex beams to participate in the reaction and the core–shell structure latex is formed.

Figure 4 shows typical TEM images of the silica sol (Fig. 4a) and silica sol/fluoroacrylate nanocomposite emulsion latex particles (Fig. 4b) which were prepared by the conventional emulsion polymerization. As shown in Fig. 4a, the size of SiO<sub>2</sub> particles is about 30–35 nm and possess narrow size-distribution. According to the Fig. 4b, the silica sol/fluoroacrylate nanocomposite emulsion latex particles exhibit core–shell morphology with one or more modified silica particles located in the latex particles. And the size of the silica sol/fluoroacrylate nanocomposite emulsion latex particles is about 100–200 nm when one or more modified silica particles were located in the latex particles. The core–shell morphology is consistent with the speculated formation mechanism of silica sol/fluoroacrylate nanocomposite latex particles. However, the introduction of KH570-silica sol which has the reactive double bond on the surface of the silica sol makes the latex possess

the core–shell morphology. It is convenient to synthesize core–shell structure latex particles through emulsion polymerization using the grafting of KH-570 onto silica particles.



**Fig. 4** TEM micrograph of the silica sol (a) and silica sol/fluoroacrylate nanocomposite latex particles (b)



**Scheme 1** Formation of the core–shell structure

**Table 2** Particle sizes tested by PCS detector at set time intervals

Sample	Particle size (nm) (PDI)		
	0 day	3 months	6 months
a	53.69 (0.010)	52.45 (0.027)	53.43 (0.048)
b	53.88 (0.012)	55.11 (0.059)	54.67 (0.011)
c	82.99 (0.041)	84.72 (0.032)	81.68 (0.066)

a, the polyacrylate copolymer latex (sample No. 1); b, fluorinated polyacrylate copolymer latex (sample No. 2); c, silica sol/fluoroacrylate nanocomposite latex (sample No. 3)

### Stability of emulsion

The stability of the emulsion latexes is symbolized by testing the particle size and particle size-distribution of latex particles by PCS detector at set time intervals. And the data is shown in Table 2. Silica sol/fluoroacrylate nanocomposite emulsion prepared in this work has good dilution, heat-resistance and cold-resistance stability compared to the polyacrylate copolymer emulsion and the fluorinated polyacrylate copolymer emulsion prepared under the same polymerization technology. The lower intermolecular force of C–F group causes the adsorption of the mixed emulsifier on the latex particle surface becomes difficult. Therefore, the small latex particles tend to integrate and the large particles deposit easily [35]. In addition, probably the cross-linking effect of the modified silica makes the polymer possess high stability. Therefore, the stability including storage stability, dilution stability, heat-resistance and cold-resistance stability of the silica sol/fluoroacrylate nanocomposite emulsion is the best one compared to the polyacrylate copolymer emulsion and the fluorinated polyacrylate copolymer emulsion.

### Thermogravimetric analysis

Thermogravimetric analysis (TGA) is used to evaluate the thermal stability of the obtained emulsion films. The weight loss of polyacrylate, fluorinated polyacrylate and silica sol/fluoroacrylate nanocomposite films correspond to the decomposition of main chain. The obtained films do not exhibit obvious weight loss before the scanning temperature reaches up to 250 °C in nitrogen atmosphere, indicating that no thermal decomposition occur. According to the curve a in the Fig. 5, the film of the polyacrylate copolymer begins to decompose at 253 °C and the process ends at 447 °C. In comparison, the decomposition of the fluorinated polyacrylate copolymer film begins at 327 °C and ends at 449 °C. After introducing fluoromonomers (curve b in Fig. 5) the decomposition temperature nearly increases by 75 °C, indicating that the thermal stability of the film is modified. It is because that the C–F bond with high bond energy can shield and protect the non-fluorinated

segment. Furthermore, the weight loss of the silica sol/fluoroacrylate nanocomposite film begins at around 350 °C and ends at 453 °C (curve c in Fig. 5). It indicates that the thermal stability of the silica sol/fluoroacrylate nanocomposite film compared to the fluorinated polyacrylate copolymer film has been improved due to the introduction of modified silica. It attributes to hydrolysis and condensation products of Si-(OCH<sub>2</sub>CH<sub>3</sub>)<sub>3</sub> which improve the thermal stability of the emulsion film by the higher energy bond of Si–O. It can be concluded from Fig. 5 that the thermal stability of the polyacrylate copolymer film can be improved by introducing modified silica and fluorinated groups.

### Water resistance of emulsion films

Water absorption of the emulsion film is one of the most important parameters to measure the hydrophobic performance of the emulsion film. As shown in Table 3, the water absorption of the polyacrylate copolymer film, the fluorinated polyacrylate copolymer film and the silica sol/fluoroacrylate nanocomposite film are 20.02, 17.53 and 12.48 %, respectively. It is due to the stronger hydrophobic properties of fluorine alkyl and silicon alkyl (silane), especially when the hydrogen atom on the main chain is substituted by the fluorine atom which has the low polarizability and the strong electronegativity. Fluorine atoms

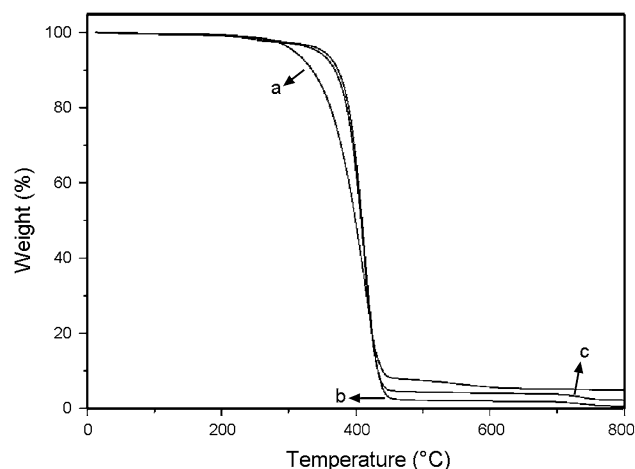


**Fig. 5** TGA curves of the polyacrylate copolymer film (a), fluorinated polyacrylate copolymer film (b) and silica sol/fluoroacrylate nanocomposite film (c) in nitrogen atmosphere

**Table 3** Water absorption of nanocomposite films

Polymer	a	b	c
Water absorption (%)	20.02	17.53	12.48

a, polyacrylate copolymer film; b, fluorinated polyacrylate copolymer film; c, silica sol/fluoroacrylate nanocomposite film



produce shield effect to the main carbon chain, thus increasing the hydrophobicity of the emulsion membranes.

### Contact angles

To investigate the surface hydrophobicity of the latex films, dynamic contact angle of water on the emulsion films is used to evaluate the hydrophobicity of the resulted films. The contact angles of water on the latex films are listed in Table 4. It can be seen that when the fluorinated monomer is introduced into the polymer chains, the fluorinated polyacrylate copolymer film shows higher contact angle compared with the polyacrylate copolymer film, as expected. The incorporation of fluorinated moieties into a polymer film results in the increase in the hydrophobicity of the latex surface. In addition, the contact angle of the silica sol/fluoroacrylate nanocomposite film increases from 81.3° to 94.5° as the hydrophobic silicon groups is introduced into the system. The contact angle measurements indicate that the hydrophobicity of the latex film has been modified by the introduction of both high hydrophobic fluorinated and silicon groups.

### UV–vis spectroscopy analysis

The Transmittance of UV–vis light through polyacrylate copolymer film, fluorinated polyacrylate copolymer film and silica sol/fluoroacrylate nanocomposite film are evaluated through UV–vis spectra which the results are depicted in Fig. 6. It can be seen from curve a in Fig. 6 that the polyacrylate copolymer film has good UV–vis transmittance at the wavelength range between 275 and 800 nm and the highest transmittance at 800 nm is up to 80 %. In comparison, the UV–vis transmittance range of the fluorinated polyacrylate copolymer film (curve b in Fig. 6) is from 290 to 800 nm and the highest transmittance is 75 % at 800 nm. Better UV–vis shielding effect of the fluorinated polyacrylate copolymer film is attributed to the existence of the C–F bonds. Bond energy of C–F bond is high enough and the fluorine atoms were concentrated in the surface of the latex film in the fluorinated polyacrylate copolymer film.

Meanwhile, the UV–vis light transmittance of the silica sol/fluoroacrylate nanocomposite film is the least according to curve c in Fig. 6. It is due to the synergistic effects of the

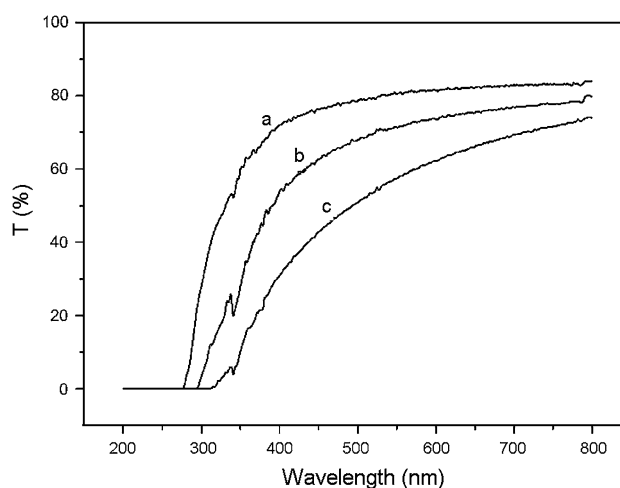


**Fig. 6** UV–vis spectra of the polyacrylate copolymer film (a), fluorinated polyacrylate copolymer film (b) and silica sol/fluoroacrylate nanocomposite film (c)

fluorine atoms which have the shielding effect to protect the backbone and the cross-linking of the modified silica which makes the emulsion film structure to be packed closely. In short, the shielding UV–vis effect of the polyacrylate copolymer film is greatly modified by the introduction of fluorinated monomer and modified silica particles.

### Conclusion

It is convenient to synthesize core–shell structure silica sol/fluoroacrylate nanocomposite latex particles through emulsion polymerization using the grafting of KH-570 onto silica particles. The existence of modified silica particles in the organic phase results in the formation of latex particles with core–shell structure. TEM micrographs reveal that the silica sol/fluoroacrylate nanocomposite latex particles exhibit core–shell morphology with one or more modified silica particles located inside the latex particles. The core–shell morphology is consistent with the speculated formation mechanism of silica sol/fluoroacrylate nanocomposite latex particles. The particle size of the core–shell latexes increases with increasing the amount of modified silica particles which is consistent with the results of PCS measurement. The storage stability, dilution stability, heat-resistant stability and cold-resistant stability of the final latex are significantly appropriate. Compared with the fluorinated polyacrylate copolymer film, the silica sol/fluoroacrylate nanocomposite film exhibits lower water absorption and higher water contact angle, which indicate its higher hydrophobic property. Furthermore, the thermal stability of the core–shell silica sol/fluoroacrylate nanocomposite film is improved with the introduction of the

**Table 4** Contact angles of water on nanocomposite films

Polymer	a	b	c
Contact angles of water (degree)	68.8	81.3	94.5

a, polyacrylate copolymer film; b, fluorinated polyacrylate copolymer film; c, silica sol/fluoroacrylate nanocomposite film





fluorinated monomer and the modified silica particles. Meanwhile, the films also possess the ability of shielding UV–vis light. The excellent hydrophobicity, thermodynamic and resistance to ultraviolet light properties endow the silica sol/fluoroacrylate nanocomposite film with potential applications in variety of fields.

**Acknowledgments** This research was financially supported by the Innovation Group Foundation of Hubei Province (No. 2006ABC012) Hubei, China. Authors also acknowledge the Ministry-of-Education Key Laboratory for the Green Preparation and Application of Functional Materials for providing necessary facilities.

## References

- Hayashida K, Tanaka H, Watanabe O (2009) Miscible blends of poly(butyl methacrylate) densely grafted on fumed silica with poly(vinyl chloride). *Polymer* 50:6228–6234
- Wen XF, Li MZ, Pi PH, Chen J, Yang ZR (2008) Study of the physicochemical properties of silica powder and the stability of organic-inorganic hybrid emulsion in the presence of ethanol. *Colloid Surface A* 327:103–110
- Deng TS, Zhang JY, Zhu KT, Zhang QF, Wu JL (2010) Highly monodisperse vinyl functionalized silica spheres and their self-assembled three-dimensional colloidal photonic crystals. *Colloid Surface A* 356:104–111
- Zhang F, Wang Y, Chai C (2004) Preparation of styrene-acrylic emulsion by using nano-SiO<sub>2</sub> as seeds. *Polym Int* 53:1353–1359
- Qi DM, Bao YZ, Weng ZX, Huang ZM (2006) Preparation of acrylate polymer/silica nanocomposite particles with high silica encapsulation efficiency via miniemulsion polymerization. *Polymer* 47:4622–4629
- Ragosta G, Abbate M, Musto P, Scarinzi G, Mascia L (2005) Epoxy-silica particulate nanocomposites: chemical interactions, reinforcement and fracture toughness. *Polymer* 46:10506–10516
- Zheng K, Chen L, Li Y, Cui P (2004) Preparation and thermal properties of silica-graft acrylonitrile-butadiene-styrene nanocomposites. *Polym Eng Sci* 44:1077–1082
- Zhang Q, Zhai YG, Liu FQ, Yang M, Gao G (2008) Synthesis of poly[2-methoxy-5-(2-ethylhexyloxy)-1,4-phenylenevinylene-silica] core-shell particles with a self-templating method and their fluorescent properties. *Eur Polym J* 44:3957–3962
- Wang YW, Yen CT, Chen WC (2005) Photosensitive polyimide/silica hybrid optical materials: synthesis, properties, and patterning. *Polymer* 46:6959–6967
- Caruso F, Spasova M, Susha A, Giersig M, Caruso RA (2001) Magnetic nanocomposite particles and hollow spheres constructed by a sequential layering approach. *Chem Mater* 13:109–116
- Knopp D, Tang D, Niessner R (2009) Review: bioanalytical applications of biomolecule-functionalized nanometer-sized doped silica particles. *Anal Chim Acta* 647:14–30
- Kickelbick G (2003) Concepts for the incorporation of inorganic building blocks into organic polymers on a nanoscale. *Prog Polym Sci* 28:83–114
- Lluch AV, Ferrer GG, Pradas MM (2009) Biomimetic apatite coating on P(EMA-co-HEA)/SiO<sub>2</sub> hybrid nanocomposites. *Polymer* 50:2874–2884
- Lee LH, Chen WC (2001) High-refractive-index thin films prepared from trialkoxysilane-capped poly(methyl methacrylate)-titania materials. *Chem Mater* 13:1137–1142
- Xiong PT, Lu DP, Chen PZ, Huang HZ, Guan R (2007) Preparation and surface properties of latexes with fluorine enriched in the shell by silicon monomer crosslinking. *Eur Polym J* 43:2117–2126
- Cheng XL, Chen ZX, Shi TS, Wang HY (2007) Synthesis and characterization of core-shell LIPN-fluorine-containing polyacrylate latex. *Colloid Surface A* 292:119–124
- Ameduri B, Boutevin B, Kostov G (2001) Fluoroelastomers: synthesis, properties and applications. *Prog Polym Sci* 26:105–187
- He L, Liang JY (2008) Synthesis, modification and characterization of core-shell fluoroacrylate copolymer latexes. *J Fluorine Chem* 129:590–597
- Hansen NML, Jankova K, Hvilsted S (2007) Fluoropolymer materials and architectures prepared by controlled radical polymerizations. *Eur Polym J* 43:255–293
- Kostova G, Rousseau A, Boutevina B, Pascal T (2005) Novel fluoroacrylated copolymers: synthesis, characterization and properties. *J Fluorine Chem* 126:231–240
- Cui XJ, Zhong SL, Gao Y, Wang HY (2008) Preparation and characterization of emulsifier-free core-shell interpenetrating polymer network-fluorinated polyacrylate latex particles. *Colloid Surface A* 324:14–21
- Chen LJ, Shi HX, Wu HK, Xiang JP (2010) Preparation and characterization of a novel fluorinated acrylate resin. *J Fluorine Chem* 131:731–737
- Lee JR, Jin FL, Park SJ, Park JM (2004) Study of new fluorine-containing epoxy resin for low dielectric constant. *Surf Coat Technol* 180–181:650–654
- Xiao XY, Wang Y (2009) Emulsion copolymerization of fluorinated acrylate in the presence of a polymerizable emulsifier. *Colloids Surface A* 348:151–156
- Li J, Fu J, Cong Y, Wu Y, Xue LJ, Han YC (2006) Macroporous fluoropolymeric films templated by silica colloidal assembly: a possible route to super-hydrophobic surfaces. *Appl Surf Sci* 252:2229–2234
- Saidi S, Guittard F, G ribaldi S (2002) Monomers reactivity ratios of fluorinated acrylates-styrene copolymers. *Polym Int* 51:1058–1062
- Lazzari M, Chiantore O, Castelvetro V (2001) Photochemical stability of partially fluorinated acrylic protective coatings: Part 3. copolymers of 1H,1H,2H,2H-perfluorodecyl acrylate and 2,2,2-trifluoroethyl methacrylate with butyl methacrylate. *Polym Int* 50:863–868
- Xiong SD, Guo XL, Li L, Wu SL, Chu PK, Xu ZS (2010) Preparation and characterization of fluorinated acrylate copolymer latexes by miniemulsion polymerization under microwave irradiation. *J Fluorine Chem* 131:417–425
- Pu FR, Williams RL, Markkula TK, Hunt JA (2002) Effects of plasma treated PET and PTFE on expression of adhesion molecules by human endothelial cells in vitro. *Biomaterials* 23:2411–2428
- Liao WB, Qu JQ, Li Z, Chen HQ (2010) Preparation of organic/inorganic hybrid polymer emulsions with high silicon content and sol-gel-derived thin films. *Chin J Chem Eng* 18:156–163
- Qu AL, Wen XF, Pi PH, Cheng J, Yang ZR (2008) Synthesis of composite particles through emulsion polymerization based on silica/fluoroacrylate-siloxane using anionic reactive and nonionic surfactants. *J Colloid Interf Sci* 317:62–69
- St ber W, Fink A, Bohn E (1968) Controlled growth of monodisperse silica spheres in the micron size range. *J Colloid Interf Sci* 26:62–69
- Philipse AP, Vrij A (1989) Preparation and properties of non-aqueous model dispersions of chemically modified, charged silica spheres. *J Colloid Interf Sci* 128:121–136



34. Cui XJ, Zhong SL, Yan J, Wang CL, Zhang HT, Wang HY (2010) Synthesis and characterization of core-shell SiO<sub>2</sub>-fluorinated polyacrylate nanocomposite latex particles containing fluorine in the shell. *Colloid Surface A* 360:41–46
35. Chen YJ, Cheng SY, Wang YF, Zhang CC (2006) Chemical components and properties of core-shell acrylate latex containing fluorine in the shell and their films. *J Appl Polym Sci* 99:107–114

